



The effect of some transition metal oxides on the physical properties of $K_{0.5}Na_{0.5}Nb_{0.95}Ta_{0.05}O_3$ ceramics

Ahmed I. Ali, M. M. Ahmed & A. Hassen

To cite this article: Ahmed I. Ali, M. M. Ahmed & A. Hassen (2016): The effect of some transition metal oxides on the physical properties of $K_{0.5}Na_{0.5}Nb_{0.95}Ta_{0.05}O_3$ ceramics, Philosophical Magazine, DOI: [10.1080/14786435.2016.1245882](https://doi.org/10.1080/14786435.2016.1245882)

To link to this article: <http://dx.doi.org/10.1080/14786435.2016.1245882>



Published online: 14 Oct 2016.



Submit your article to this journal [↗](#)



View related articles [↗](#)



View Crossmark data [↗](#)

The effect of some transition metal oxides on the physical properties of $K_{0.5}Na_{0.5}Nb_{0.95}Ta_{0.05}O_3$ ceramics

Ahmed I. Ali^{a,c}, M. M. Ahmed^d and A. Hassen^b

^aDepartment of Physics and Energy Harvest-Storage Research Center (EHSRC), University of Ulsan, Ulsan, South Korea; ^bFaculty of Science, Department of Physics, Fayoum University, El Fayoum, Egypt; ^cFaculty of Industrial Education, Basic Science Department, Helwan University, Cairo, Egypt; ^dFaculty of Engineering in Mattered, Mathematics and Physics Engineering Department, Helwan University, Cairo, Egypt

ABSTRACT

Both $K_{0.5}Na_{0.5}Nb_{0.95}Ta_{0.05}O_3$ (KNNTO) and $(K_{0.5}Na_{0.5}Nb_{0.95}Ta_{0.05}O_3)_{3-0.99}M_{0.01}$, $M = Co_3O_4$ and Mn_2O_3 (M /KNNTO) Ferromagnetic behaviour was observed for some M /KNNTO compounds. The hardness and compressive strength of all investigated samples are given. Comparisons with similar materials are discussed. Ceramics were synthesised using a solid-state reaction method. X-ray diffraction patterns of all samples revealed that the crystal structure is orthorhombic. Field-emission scanning electron microscopy was performed. Polarisation hysteresis curves indicated a disruption of ferroelectric order with the addition of M into KNNTO ceramics. The dielectric properties of the investigated ceramics have been studied as a function of frequency and temperature.

ARTICLE HISTORY

Received 28 June 2016
Accepted 4 October 2016

KEYWORDS

Lead-free materials;
characterisation;
ferroelectricity;
magnetisation; dielectric
properties; hardness and
compressive strength

1. Introduction

Multiferroic materials combine two or more ferroic properties, such as ferromagnetism and ferroelectricity. Ferroelectricity is important for random-access memory (RAM) [1] and leads to piezoelectricity, which finds use in applications such as sensors, transducers and actuators because of its ability to couple electrical and mechanical displacements. This means that the electrical polarisation changes in response to an applied mechanical stress and/or mechanical strain can respond to an applied electric field. Some materials have recently attracted more attention because of the need for high piezoelectric sensitivity and lead-free composition [2–4]. The development of materials with high piezoelectric sensitivity and lead-free composition is still a major scientific challenge, driven by both the toxicity of lead oxide (PbO) and directives for environmental protection. Therefore, the elimination of PbO from the composition of ferro-piezoelectric ceramics in devices becomes a directive requirement. On the other hand, ferromagnetic properties are useful for recording devices, transforms and the magnetic strip on the back of credit cards. Therefore, taking information

in the form of electrical signals and encoding it into magnetic materials makes multiferroics an active area of research.

Generally, most ferroelectrics are transition metal oxides, in which transition ions exhibiting an empty d shell seem to be a prerequisite for ferroelectricity [5]. In contrast, magnetism requires transition ions with partially filled d -shells, such as Mn^{3+} and Fe^{3+} ions. The difference in the d shells required for the ferroelectricity and magnetism makes these two orders mutually exclusive. This explains the difficulty associated with the coexistence of ferroelectricity and ferromagnetism. But some compounds, such as BiMnO_3 and BiFeO_3 , show simultaneous ferromagnetism and ferroelectricity [4,6]. In these compounds, ferromagnetic and ferroelectric properties are associated with different ions, i.e. $\text{Mn}^{3+}/\text{Fe}^{3+}$ and Bi^{3+} , respectively. In most multiferroic materials, one cation should produce ferroelectricity and the other produce ferromagnetism. Various studies have been carried out according to this idea [7–10]. For instance, introducing magnetic ions (Fe ions) into BaTiO_3 leads to the coexistence of ferroelectricity and ferromagnetism at room temperature [7]. In addition, the magnetoelectric effect of $\text{Pb}(\text{Fe}_x\text{Ti}_{1-x})\text{O}_3$ has been reported by Palkar and Malik [8].

Recently, potassium–sodium–niobate tantalate compound, $\text{K}_{0.5}\text{Na}_{0.5}\text{Nb}_{0.95}\text{Ta}_{0.05}\text{O}_3$, (KNNTO) has been investigated as a lead-free piezoelectric material. It has excellent piezoelectric and ferroelectric properties [11–19] in addition to its chemical interest [20]. Similar to BaTiO_3 and lead zirconate titanate (PZT), introducing magnetic ions such as Mn, Co or Fe to KNNTO-based materials could cause the coexistence of ferroelectricity and ferromagnetism and further the coupling between them. Li et al. [21] reported on the magnetocapacitance of Fe-doped KNNTO. They emphasised that Fe-doped KNNTO revealed ferroelectric and magnetic properties simultaneously. In addition, there is a coupling between ferroelectric and ferromagnetic orders in Fe-doped ceramics with the application of a magnetic field because a clear change in dielectric constant is observed. These results revealed that Fe-doped KNNTO materials could be a promising candidate for practical applications.

It was reported that the Curie temperature, T_C , of the KNNTO ceramics depends on the sintering temperature, S_T , and it is 380 °C at $S_T = 1120$ °C [15]. Peddigari and Dobbidi [22] studied the dielectric properties of Gd_2O_3 -doped $\text{K}_{0.5}\text{Na}_{0.5}\text{NbO}_3$ (KNNO). They reported that the T_C of KNNO is 374 °C. Doping KNNO by Gd_2O_3 enhanced its dielectric permittivity, ϵ' , and shifted the polymorphic phase transition orthorhombic to tetragonal transition temperature ($T_O - T$) from 199 to 85 °C. Moreover, the effect of NaF addition on the dielectric properties of KNNTO ceramics was studied [23]. It was found that the NaF doping does not affect the phase transition temperatures of KNNTO significantly, with $T_O - T = 180$ °C and $T_C = 380$ °C.

This work aims to synthesise ceramics of pure KNNTO and $(\text{K}_{0.5}\text{Na}_{0.5}\text{Nb}_{0.95}\text{Ta}_{0.05}\text{O}_3)_{0.99}\text{-M}_{0.01}$ (M/KNNTO), where $M = \text{Mn}_2\text{O}_3$, and Co_3O_4 , using a solid-state reaction method. Then, the crystal structure of the investigated compounds is examined. Characterisation technique, such as field-emission scanning electron microscopy (FE-SEM), was utilised to test the particle size. In addition, the effect of both metal transition oxides on ferroelectric as well as the magnetic properties of KNNTO was performed. Also, the temperature and frequency dependences of both dielectric permittivity (ϵ') and losses ($\tan \delta$) of the studied samples are discussed. We observed an enhancement of both ferroelectricity and magnetism in the investigated samples.

2. Experimental

The $K_{0.5}Na_{0.5}Nb_{0.95}Ta_{0.05}O_3$ and $(K_{0.5}Na_{0.5}Nb_{0.95}Ta_{0.05}O_3)_{0.99}M_{0.01}$, with $M = Mn_2O_3$ and Co_3O_4 , ferroelectric ceramics were synthesised by a conventional solid-state technique using K_2CO_3 , Na_2CO_3 , Ta_2O_5 (99.9% High Purity Chemicals, Japan) and Nb_2O_5 (99.9% Cerac Specialty In-organics, USA) as starting raw materials. Before weighing, the powders were dried in an oven at 100 °C for 24 h to eliminate moisture. The starting materials were mixed according to the stoichiometric formula and ball-milled for 24 h in ethanol with zirconia balls. The dried slurry was ground and calcined at 750 °C for 2 h, followed by another ball-milling for 24 h. The powders were pulverised and pressed into discs with diameters of 12 mm at 100 MPa.

Sintering was carried out in the temperature range of 1050–1100 °C for 2 h in covered alumina crucibles. To prevent the vaporisation of Na and K, the discs were embedded in a powder of the corresponding composition. X-ray powder diffraction (XRD) was performed using a Rigaku Co-Miniflex X-ray diffractometer employing CuK_{α} radiation with $\lambda = 1.5418 \text{ \AA}$. The microstructures of ceramic samples were analysed with a field-emission scanning electron microscope (FE-SEM; JEOL, JSM-65 OFF). Ferroelectric hysteresis loops were measured in silicon oil with the aid of a Sawyer–Tower circuit to apply an electric field with a sinusoidal waveform. DC magnetisation measurements were performed in a SQUID magnetometer (Quantum design MPMS5S). To accurately observe the behaviour of each sample, measurements of dc magnetization-applied field ($M-H$) curves were measured at 10 K. Dielectric measurements were performed using a Hioki (Ueda, Nagano, Japan) model 3532 High Tester LCR, with a capacitance measurement accuracy on the order of 0.0001 pF. The temperature was measured with a T -type thermocouple having an accuracy of ± 1 °C. The dielectric permittivity, ϵ' , of each sample was calculated as $\epsilon' = dC/\epsilon_0 A$, where C is the capacitance, d is the thickness of the sample, ϵ_0 is the permittivity of free space and A is the cross-sectional area of the sample. Also, $\tan \delta = \epsilon''/\epsilon'$, where ϵ'' is the dielectric losses. The average crushing strength was tested by compressing 10 briquettes between parallel steel plates to their breaking point using a MEGAKSC-10 hydraulic press. The hardness was determined using a Vickers Hardness Tester (HVB-30 A).

3. Results and discussion

3.1. Characterisation

Polycrystalline samples of KNNTO and M /KNNTO, where M is Mn_2O_3 , Co_3O_4 and $\alpha-Fe_2O_3$, were characterised by powder XRD at room temperature, as shown in Figure 1(a). All reflection peaks characterise an orthorhombic structure without any residuals of the original constituent oxides, indicating that most of the induced ions diffuse into the host lattice. The M /KNNTO ceramics exhibit a splitting in the (200)/(002) diffraction peaks as shown in Figure 1(b). This splitting is small but it can be seen compared with pure KNNTO, confirming the slight effect of doping oxides on the structure of the mother compound. As also shown in Figure 1(b), the position of either (200) or (002) diffraction peaks of M /KNNTO samples is the same. The lattice parameters and unit cell volume of the investigated samples are listed in Table 1. The values of the lattice parameters are consistent with those of similar compounds [24]. Because the ionic radii at the A -site of KNNTO (Na^+ : 0.102 nm and K^+ : 0.138 nm) are larger than those at its B -site (Nb^{5+} : 0.069 nm and Ta^{5+} : 0.068 nm) [12,13],

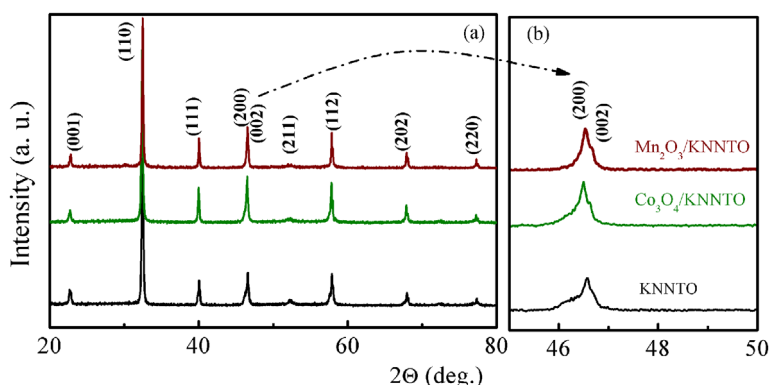


Figure 1. (colour online) (a) X-ray diffraction patterns, XRD, of pure KNNTO and M/KNNTO samples. (b) An enlargement of the (200)/(002) diffraction peaks.

Table 1. The lattice parameters and average particle size of KNNTO and M/KNNTO ceramic samples.

Sample	a (Å)	b (Å)	c (Å)	V (Å ³)	Average particle size (μm)
KNNTO	17.3240	17.5870	3.9242	1195.61422	2.02
Co ₃ O ₄ /KNNTO	17.3240	17.5870	3.9190	1194.0299	3.10
Mn ₂ O ₃ /KNNTO	17.3240	17.5870	3.9267	1196.37591	3.34

the M ions probably substitute at the B -site, (Ta^{5+}/Nb^{5+}). The ionic radii of doped ions are Mn^{3+} : 0.0645 nm [25], and Co^{3+} : 0.061 nm [26]. It seems that our doped ions are suitable for substitution at the B -site, i.e. the Nb and Ta ions. Because there is a small difference between the ionic radii of M ions and Nb/Ta, the change in the lattice parameters a , b with doping is small. The lattice parameter c changes slightly with doping. Using the XRD results, the grain size (D) was calculated using the well-known Scherrer equation, $D = 0.9\lambda / (B \cos \theta)$, where B is the full width at half maximum intensity (FWHM) in radians, θ is the Bragg's angle and $\lambda = 1.54$ Å. The average grain size of KNNTO is 2.02 μm and changes according to the doped metal oxide, as seen in Table 1.

Figure 2(a)–(c) shows FE-SEM images of KNNTO and M/KNNTO ceramic samples. The surface images show that all grains are rectangular or cubic. The parent sample primarily consists of grains with sizes of 1–2.96 μm. With doping, large grains become common, depending on the type of ion. This reveals that the addition of M is effective for promoting grain growth. The estimation of particle size deduced from XRD data is consistent with that observed from FE-SEM.

3.2. Ferroelectric and magnetic properties

The P – E loops were traced for all samples, as presented in Figure 3(a)–(c). There are no complete saturation polarisations within the studied electric field range. Further attempts to reach full saturation were not attempted because of electrical breakdown when E exceeded 2 kV/mm. It is noticed that P – E loops for KNNTO is asymmetry compared to those of other two investigated ceramic samples. This behaviour is the result of building up of the internal bias field, which plays an important role in the properties of ceramics [27–29]. The

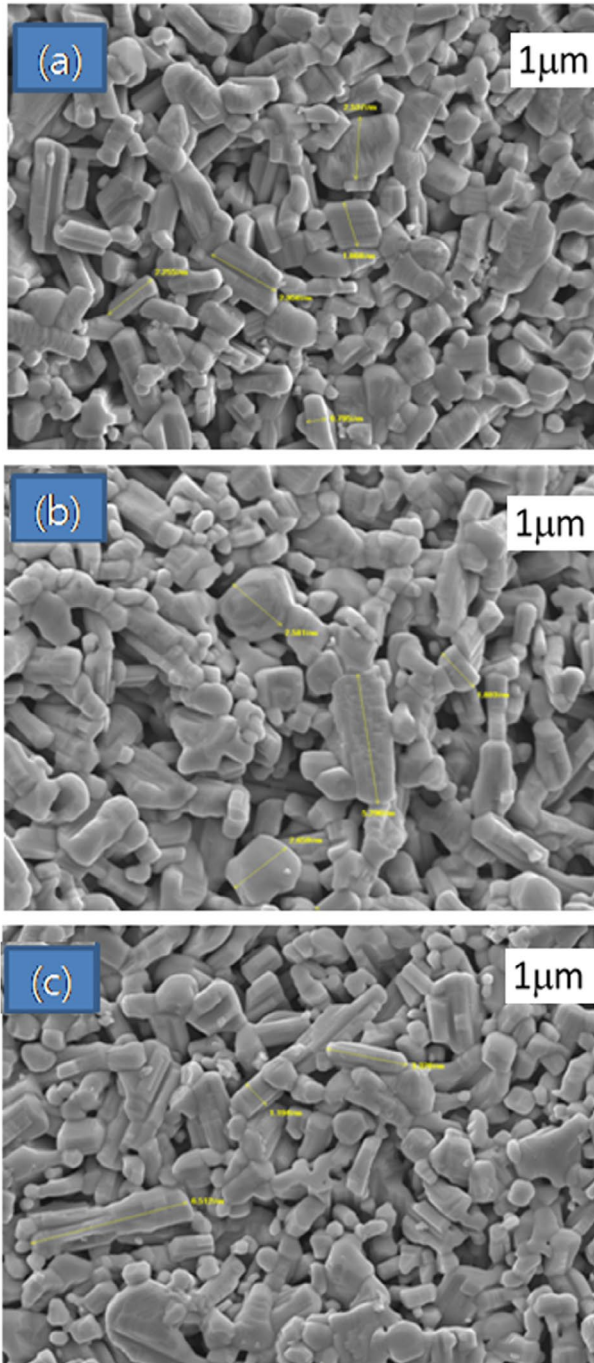


Figure 2. (colour online) The FE-SEM images for polycrystalline samples: (a) KNNTO, (b) Co₃O₄/KNNTO, and (c) Mn₂O₃/KNNTO.

mechanisms responsible for the occurrence of an internal bias in the lead-free ferroelectrics are based on the stabilisation of domain wall movement. The maximum polarisation (P_{\max})

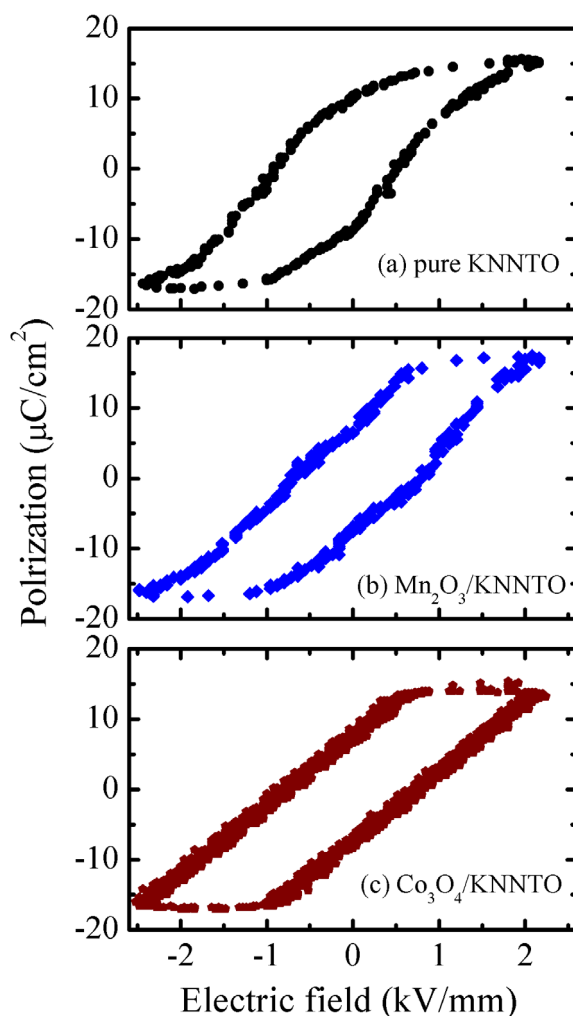


Figure 3. (colour online) P - E hysteresis loops at room temperature for ceramic samples: (a) KNNTO, (b) $\text{Co}_3\text{O}_4/\text{KNNTO}$, and (c) $\text{Mn}_2\text{O}_3/\text{KNNTO}$.

Table 2. The physical properties of KNNTO and M/KNNTO polycrystalline samples, listed are: maximum polarization, P_{max} , maximum magnetic moment, compressive strength, and hardness.

Physical parameters	KNNTO	$\text{Co}_3\text{O}_4/\text{KNNTO}$	$\text{Mn}_2\text{O}_3/\text{KNNTO}$
P_{max} ($\mu\text{C}/\text{cm}^2$)	15.37	13.6	17.46
Maximum magnetization $\times 10^{-4}$ (emu/mass)	1.768	1.782	137
Compressive strength (MPa)	18.73	23.41	14.05
Hardness (MPa)	34.4	38.4	34.6

for each sample was calculated and is listed in Table 2. It is clear that the values of P_{max} as well as the area of the hysteresis depend on M . In other words, the ferroelectricity of KNNTO was affected by adding 1.0 wt.% of M . Moreover, KNNTO tends to be a hard ferroelectric when a small amount of Co_3O_4 adds to it. The ferroelectric behaviour of KNNTO seems to

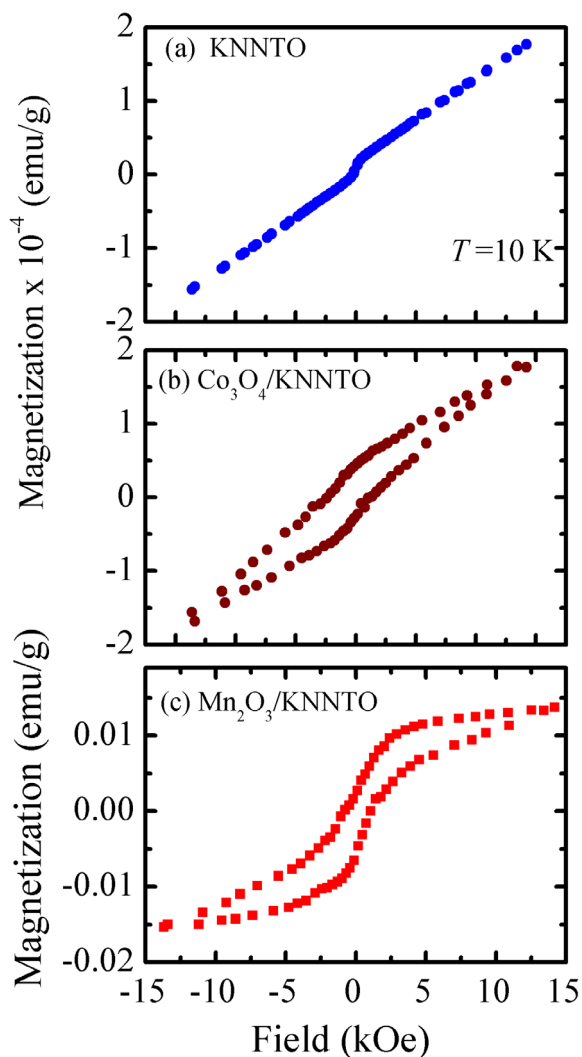


Figure 4. (colour online) Mass magnetisation versus applied magnetic field at 10 K for the studied samples: (a) KNNTO, (b) $\text{Co}_3\text{O}_4/\text{KNNTO}$, and (c) $\text{Mn}_2\text{O}_3/\text{KNNTO}$.

be affected by the doping of transition metal ions. Therefore, a change in magnetic behaviour of KNNTO is expected as seen in the next figure.

Figure 4(a)–(c) depicts the specific magnetisation of all samples versus magnetic field at 10 K. Focusing first on the KNNTO sample, paramagnetic behaviour was observed: the magnetisation increased linearly within the studied range of applied magnetic field because no hysteresis loop was observed for the mother sample, even at 10 K. On the other hand, a hysteresis loop was observed for M/KNNTO ceramics. Both the hysteresis area and the value of the magnetic moment varied according to the type of M ion. Magnetisation becomes closer to saturation for Mn-doped KNNTO than it does for Co-doped KNNTO. Similar behaviour has been reported for Fe-doped KNNTO [21]. Moreover, the maximum value of the magnetic moment of pure KNNTO and Co-KNNTO is smaller than that of Mn-doped

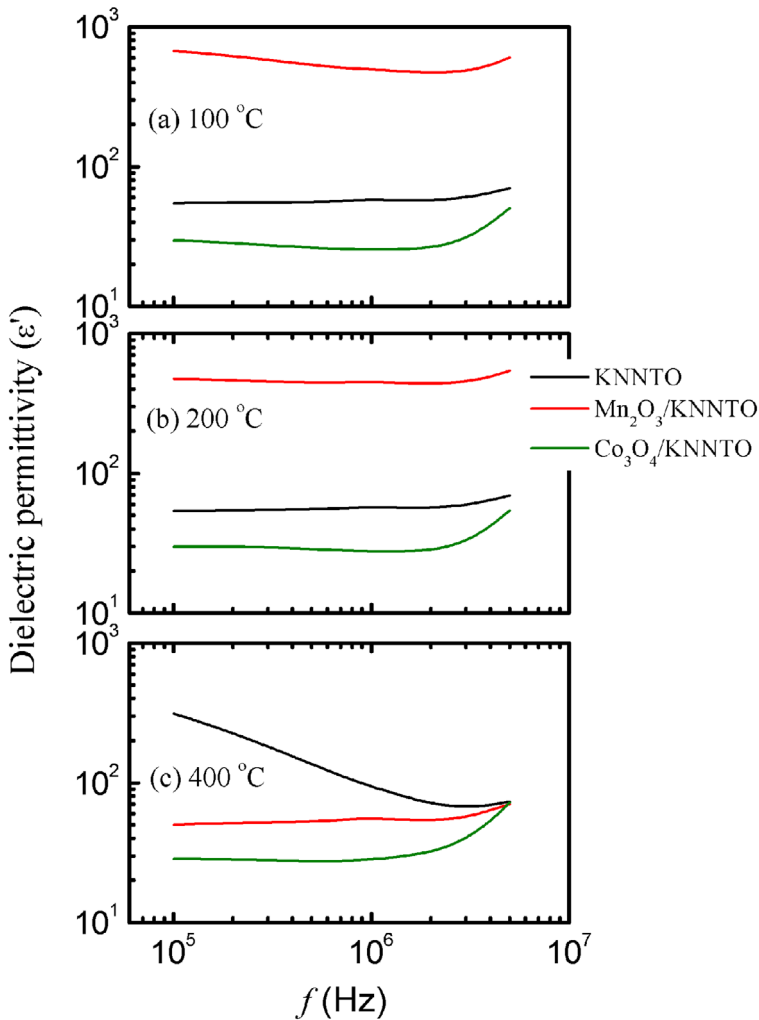


Figure 5. (colour online) Frequency dependence of the dielectric permittivity, ϵ' , for pure KNNTO and M/KNNTO at different temperatures.

KNNTO samples, as seen in Table 2. It was also found that the magnetic ordering of these ceramics exist only at low temperatures. Magnetic disorder is observed for these samples when temperature raised up. Both Mn^{3+} and Co^{3+} ions probably substitute for the Nb^{5+} ion at the *B*-site of KNNTO. This means the magnetic behaviour of *M*-doped KNNTO can be explained based on the coupling between metal transition ions and Nb ions. Similar behaviour was reported for Eu-doped BaTiO_3 [30].

3.3. Dielectric properties

Figure 5(a)–(c) represents the frequency dependence of ϵ' for pure KNNTO and KNNTO doped with Co_3O_4 and Mn_2O_3 . It is noticed that ϵ' decreased with increasing frequency (f) until a certain value of f and then it increased slightly depending on the T_c of each

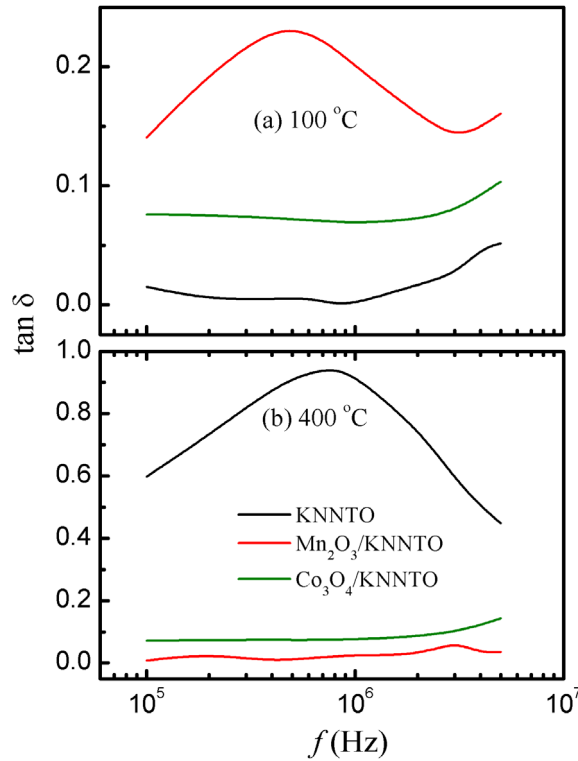


Figure 6. (colour online) Frequency dependence of $\tan \delta$ for pure KNNTO and M/KNNTO ceramics at different temperatures.

compound. When the temperature is near from the T_C of Mn_2O_3 , ϵ' exhibits higher values than those of pure KNNTO and Co_3O_4 -doped KNNTO samples (see Figure 5(a) and (b)). This means that T_C of Mn_2O_3 is lower than those of two other samples. On the other hand, ϵ' of pure KNNTO is the highest compared to M/KNNTO ceramics at $T = 400^\circ\text{C}$ as seen in panel c of Figure 5. This means that T_C of pure sample is near from such temperature similar to earlier reports [15,23]. Another evidence that Mn_2O_3 -doped KNNTO shows a lower T_C compared with those of pure KNNTO and KNNTO doped with Co_3O_4 , is the variation of $\tan \delta$ with frequency at different temperatures as shown in Figure 6. In addition, both pure KNNTO and Mn_2O_3 -doped KNNTO show peaks on contrast to Co_3O_4 -doped one [see Figure 8(a, c)]. The first peak around 100°C can be attributed to $T_O - T$ transition in M_2O_3 -doped NNTO, while the second peak for KNNTO is due to T_C .

The temperature dependence of the ϵ' for pure KNNTO and KNNTO doped with Mn_2O_3 and Co_3O_4 at different frequencies is depicted in Figure 7. It is noticed that Mn_2O_3 -doped KNNTO shows a peak around 100°C before ferroelectric transition at 200°C . This peak might be attributed to structural transition consistent with previous reports [23,31,32]. While pure KNNTO exhibits T_C around 360°C , Co_3O_4 -doped KNNTO undergoes a transition around 320°C . To emphasise these results, the variation of $\tan \delta$ against temperature at different frequencies is plotted in Figure 8. Again, a peak around 100°C is observed for Mn_2O_3 -doped KNNTO and its height changed with increasing temperature. This is another evidence that Mn_2O_3 -doped KNNTO sample exhibits $T_C \approx 200^\circ\text{C}$ consistent with the results

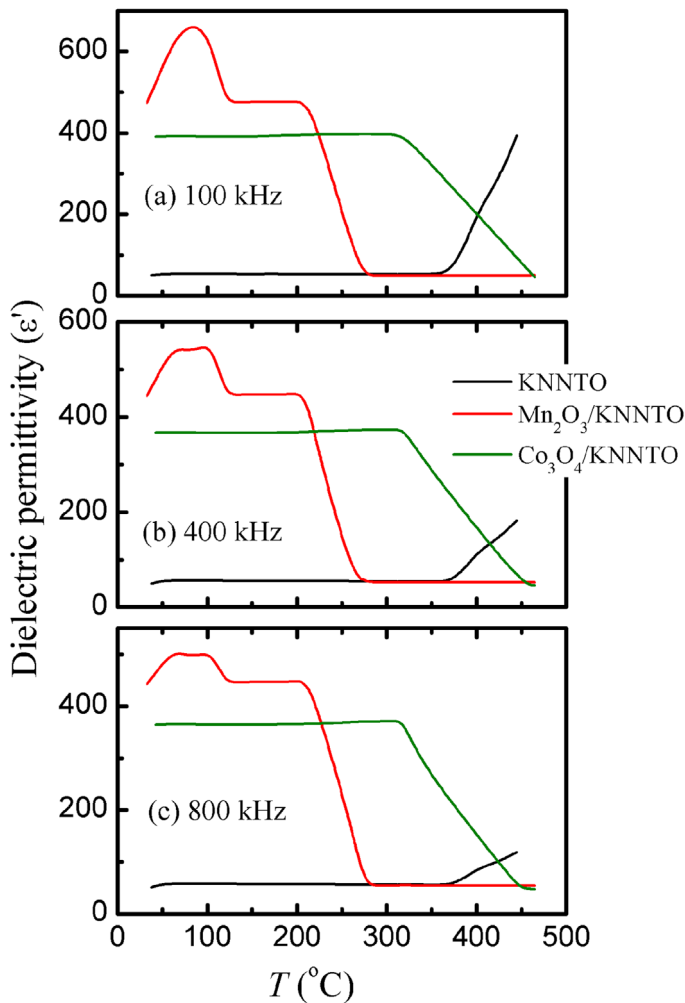


Figure 7. (colour online) Temperature dependence of the dielectric permittivity, ϵ' , for pure KNNTO and M/KNNTO at different frequencies.

of $\epsilon'(T)$. Also, the losses of pure KNNTO increased in the vicinity of $T_C \approx 360^\circ\text{C}$, and this behaviour can be seen in the inset of Figure 8(a). Concerning Co_3O_4 -doped KNNTO, there is a broad peak around 155°C may be due to structural transition. This peak shifts towards higher temperatures with increasing frequency. Compared with $\epsilon'(T)$ data, ferroelectric transition is observed in the $\text{Co}_3\text{O}_4/\text{KNNTO}$ sample around 400°C .

The values of both compressive strength and hardness of all investigated samples were determined. The results are given in Table 2. Co_3O_4 -KNNTO exhibited the highest compressive strength and hardness among the studied samples. This means that the mechanical properties of the host compound can be altered, even with a small amount of doping.

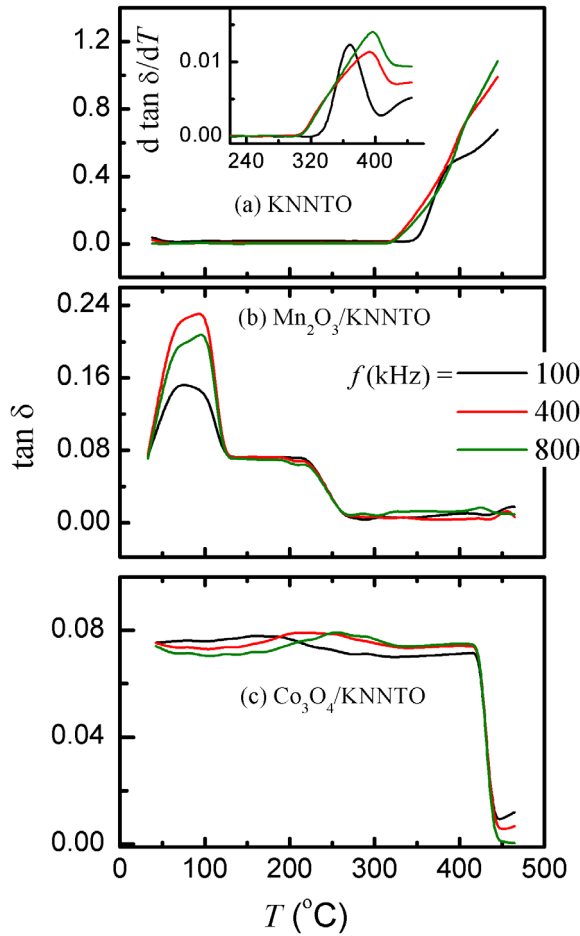


Figure 8. (colour online) Temperature dependence of $\tan \delta$ for pure KNNTO and M/KNNTO ceramics at different frequencies.

4. Conclusions

The XRD patterns at room temperature revealed that pure KNNTO and M/KNNTO compounds crystallise in an orthorhombic structure. The average particle size changed with M doping. P - E hysteresis loops showed that the maximum polarisation, P_{\max} , and hysteresis area also depend on the doped M ions. The results of mass magnetisation confirmed the existence of ferromagnetism for Mn-doped KNNTO, in addition to its ferroelectricity. On the other hand, Co-doped KNNTO exhibited a different kind of ordering compared with that of KNNTO, which shows paramagnetic behaviour, even at 10 K. Based on the dielectric results, structural transitions of doped ceramics are observed before entering their ferroelectric transition. Also, T_C of KNNTO is changed by Co_3O_4 and Mn_2O_3 dopants. Both hardness and compressive strength changed with M doping, and the Co-doped KNNTO sample has better mechanical properties than those of pure KNNTO and KNNTO doped with Mn_2O_3 . The results of this work suggest that the investigated samples would be appropriate for various applications.

Disclosure statement

No potential conflict of interest was reported by the authors.

Funding

This study was financially supported from the Faculty of Industrial Education, Helwan University, and Faculty of Science, Fayoum University, Egypt.

References

- [1] F. Rubio-Marcos, A.D. Campo, P. Marchet, and J.F. Fernández, *Ferroelectric domain wall motion induced by polarized light*, Nat. Commun. 6 (2015). doi:10.1038/ncomms7594.
- [2] K.F. Wang, J.M. Liu, and Z.F. Ren, *Multiferroicity: The coupling between magnetic and polarization orders*, Adv. Phys. 58 (2009), pp. 321–448.
- [3] J. Ma, J. Hu, Z. Li, and C.W. Nan, *Recent progress in multiferroic magnetoelectric composites: From bulk to thin films*, Adv. Mater. 23 (2011), pp. 1062–1087.
- [4] J. Wang, J.B. Neaton, H. Zheng, V. Nagarajan, S.B. Ogale, B. Liu, D. Viehland, V. Vaithyanathan, D.G. Schlom, U.V. Waghmare, N.A. Spaldin, K.M. Rabe, M. Wuttig, and R. Ramesh, *Epitaxial BiFeO₃ multiferroic thin film hetero-structures*, Science 299 (2003), pp. 1719–1722.
- [5] R.E. Cohen, *Origin of ferroelectricity in perovskite oxides*, Nature 358 (1992), pp. 136–138.
- [6] T. Kimura, S. Kawamoto, I. Yamada, M. Azuma, M. Takano, and Y. Tokura, *Magnetocapacitance effect in multiferroic BiMnO₃*, Phys. Rev. B 67 (2003), p. 180401(R).
- [7] B. Xu, K.B. Yin, J. Lin, Y.D. Xia, X.G. Wan, J. Yin, X.J. Bai, J. Du, and Z.G. Liu, *Room-temperature ferromagnetism and ferroelectricity in Fe-doped BaTiO₃*, Phys. Rev. B 79 (2009), p. 134109.
- [8] V.R. Palkar and S.K. Malik, *Observation of magnetoelectric behavior at room temperature in Pb(Fe_xTi_{1-x})O₃*, Solid State Commun. 134 (2005), pp. 783–786.
- [9] Z. Ren, G. Xu, X. Wei, Y. Liu, X. Hou, P. Du, W. Weng, G. Shen, and G. Han, *Room-temperature ferromagnetism in Fe-doped PbTiO₃ nanocrystals*, Appl. Phys. Lett. 91 (2007), pp. 063103–063106.
- [10] S. Puthucheri, P.K. Pandey, N.S. Gajbhiye, A. Gupta, A. Singh, R. Chatterjee, and S.K. Date, *Microstructural, electrical, and magnetic properties of acceptor-doped nanostructured lead zirconate titanate*, J. Am. Ceram. Soc. 94 (2011), pp. 3941–3947.
- [11] K. Wang, J. Li, and J. Zhou, *High normalized strain obtained in Li-modified (K, Na)NbO₃ lead-free piezoceramics*, Appl. Phys. Express 4 (2011), pp. 061501–061503.
- [12] E. Li, H. Kakemoto, S. Wada, and T. Tsurumi, *Influence of CuO on the structure and piezoelectric properties of the alkaline niobate-based lead-free ceramics*, J. Am. Ceram. Soc. 90 (2007), pp. 1787–1791.
- [13] W. Yang, Z. Zhou, B. Yang, R. Zhang, Z. Wang, H. Chen, and Y. Jiang, *Structure and piezoelectric properties of Fe-doped potassium sodium niobate tantalate lead-free ceramics*, J. Am. Ceram. Soc. 94 (2011), pp. 2489–2493.
- [14] R. Zuo, Z. Xu, and L. Li, *Dielectric and piezoelectric properties of Fe₂O₃-doped (Na_{0.5}K_{0.5})_{0.96}Li_{0.04}Nb_{0.86}Ta_{0.1}Sb_{0.04}O₃ lead-free ceramics*, J. Phys. Chem. Sol. 69 (2008), pp. 1728–1732.
- [15] C.-M. Cheng, K.-H. Chen, H.-C. Yang, C.-F. Yang, W.-C. Tzou, M.-C. Kuan, and F.-C. Jong, *Dielectric characteristics of the lead-free piezoelectric ceramics K_{0.50}Na_{0.50}Nb_{0.95}Ta_{0.05}O₃*, Key Eng. Mater. 434–435 (2010), pp. 285–288.
- [16] X. Wang, J. Wu, D. Xiao, J. Zhu, X. Cheng, T. Zheng, B. Zhang, X. Lou, and X. Wang, *Giant piezoelectricity in potassium–sodium niobate lead-free ceramics*, J. Am. Chem. Soc. 136 (2014), pp. 2905–2910.
- [17] X. Huo, R. Zhang, L. Zheng, S. Zhang, R. Wang, J. Wang, S. Sang, B. Yang, and W. Cao, *(K, Na, Li)(Nb, Ta)O₃: Mn lead-free single crystal with high piezoelectric properties*, J. Am. Ceram. Soc. 98 (2015), pp. 1829–1835.

- [18] F. Rubio-Marcos, P. Ochoa, and J.F. Fernandez, *Sintering and properties of lead-free (K, Na, Li) (Nb, Ta, Sb)O₃ ceramics*, J. Eur. Ceram. Soc. 27 (2007), pp. 4125–4129.
- [19] F. Rubio-Marcos, A.D. Campo, R. López-Juárez, J.J. Romeroa, and J.F. Fernández, *High spatial resolution structure of (K, Na)NbO₃ lead-free ferroelectric domains*, J. Mater. Chem. 22 (2012), pp. 9714–9720.
- [20] J. Wu, D. Xiao, and J. Zhu, *Potassium–sodium niobate lead-free piezoelectric materials: Past, present, and future of phase boundaries*, Chem. Rev. 115 (2015), pp. 2559–2595.
- [21] H. Li, W. Yang, Y. Li, Q. Meng, and Z. Zhou, *Room-temperature magnetocapacitance in Fe-doped K_{0.5}Na_{0.5}Nb_{0.95}Ta_{0.05}O₃ ceramics*, Appl. Phys. Express 5 (2012), p. 101501.
- [22] M. Peddigari and P. Dobbidi, *Raman, dielectric and variable range hopping nature of Gd₂O₃-doped K_{0.5}N_{0.5}NbO₃ piezoelectric ceramics*, AIP Adv. 5 (2015), p. 107129.
- [23] H. Li, D. Gong, W. Yang, and Z. Zhou, *Microstructure and piezoelectric properties of NaF-doped K_{0.5}Na_{0.5}Nb_{0.95}Ta_{0.05}O₃ lead-free ceramics*, J. Mater. Sci. 48 (2013), pp. 1396–1400.
- [24] D. Atencio, R.R.C. Filho, S.J.M. Mills, J.M.V. Coutinho, S.B. Honorato, A.P. Ayala, J. Ellena, and M.B.D. Andrade, *Rankamaite from the Urubu pegmatite, Itinga, Minas Gerais, Brazil: Crystal chemistry and Rietveld refinement*, Am. Mineral. 96 (2011), pp. 1455–1460.
- [25] R.D. Shannon, *Revised effective ionic radii and systematic studies of interatomic distances in halides and chalcogenides*, Acta Crystallogr. Sect. A 32 (1976), pp. 751–767.
- [26] K. Knízek, J. Hejtmánek, M. Maryško, Z. Jirák, and J. Buršík, *Stabilization of the high-spin state of Co³⁺ in LaCo_{1-x}Rh_xO*, Phys. Rev. B 85 (2012), pp. 134401–134407.
- [27] S. Takahashi, *Effects of impurity doping in lead zirconate–titanate ceramics*, Ferroelectrics 41 (1982), pp. 143–156.
- [28] K.H. Hardtl, *Electrical and mechanical losses in ferroelectric ceramics*, Ceram. Int. 8 (1982), pp. 121–127.
- [29] K. Okazaki and H. Maiwa, *Space charge effects on ferroelectric ceramic particle surfaces*, Jpn. J. Appl. Phys. 31 (1992), pp. 3113–3116.
- [30] K.Z. Rushchanskii, S. Kamba, V. Goian, P. Vaněk, M. Savinov, J. Prokleška, D. Nuzhnyy, K. Knízek, F. Laufek, S. Eckel, S.K. Lamoreaux, A.O. Sushkov, M. Ležai, and N.A. Spaldin, *A multiferroic material to search for the permanent electric dipole moment of the electron*, Nat. Mater. 9 (2010), p. 649.
- [31] R. López, F. González, M.P. Cruz, and M.E. Villafuerte-Castrejon, *Piezoelectric and ferroelectric properties of K_{0.5}Na_{0.5}NbO₃ ceramics synthesized by spray drying method*, Mater. Res. Bull. 46 (2011), pp. 70–74.
- [32] J. Wang, L. Luo, Y. Huang, W. Li, and F. Wang, *Strong correlation of the electrical properties, up-conversion photoluminescence, and phase structure in Er³⁺/Yb³⁺ co-doped (1-x) K_{0.5}Na_{0.5}NbO_{3-x}LiNbO₃ ceramics*, Appl. Phys. Lett. 107 (2015), p. 192901.